# Distinct developmental mechanisms influence sexual dimorphisms in the milkweed bug *Oncopeltus fasciatus*

Josefine Just [†,1,2], Mara Laslo [†,2], Ye Jin Lee [1], Michael Yarnell [4], Zhuofan Zhang [5], David R. Angelini *[, 1]

[†] These authors contributed equally.

* Corresponding author email: david.r.angelini@gmail.com

**ORCID**

| | |
|---|---|
| 0000-0002-5342-518X | Josefine Just [1, 2] |
| 0000-0003-4022-4327 | Mara Laslo [1, 3] |
| 0000-0002-9100-5282 | Ye Jin Lee [1] |
| 0000-0002-4557-7255 | Michael Yarnell [4] |
| 0000-0003-2269-3859 | Zhuofan Zhang [1, 5] |
| 0000-0002-2776-2158 | David R. Angelini [1] |

[1] Department of Biology, Colby College, 5700 Mayflower Hill, Waterville, ME 04901
[2] Department of Organismic & Evolutionary Biology, Harvard University, 16 Divinity Avenue, Cambridge, MA 02138
[3] Department of Stem Cell and Regenerative Biology, Harvard University, 7 Divinity Avenue, Cambridge, MA 02138
[4] Department of Pediatrics, University of Colorado School of Medicine, 13123 E. 16th Ave., B065, Aurora, CO 80045
[5] School of Electrical and Computer Engineering, Georgia Institute of Technology, 777 Atlantic Dr, Atlanta, GA 30332

**Keywords**
Sexual dimorphism; sex determination; *doublesex*; *intersex*; *fruitless*; alternative splicing

**Author contributions**

- JJ and ML designed and conducted most experiments and contributed equally to data analysis, creation of draft figures, and writing of the main text.
- YJL, MY, and ZZ conducted portions of the experiments and contributed to data analysis.
- DRA designed and supervised all experiments, secured funding, prepared final figures, and contributed to data analysis and to the writing of the main text.

# Abstract

Sexual dimorphism is a common feature of animals. Sex determination mechanisms vary widely and evolve rapidly. In sexually dimorphic cells throughout the body of *Drosophila*, the relative dosage of autosomes and X chromosomes leads indirectly to alternatively spliced transcripts from the gene *doublesex*. The female Dsx isoform interacts with the mediator complex protein encoded by *intersex* to activate female development in flies. In males the transcription factor encoded by *fruitless* promotes male-specific behavior. In the milkweed bug *Oncopeltus fasciatus*, we find a requirement for different combinations of these genes during development of distinct dimorphic structures, within the same sex, suggesting a previously unappreciated level of diversity in sex determination. While *intersex* and *fruitless* are structurally conserved, *doublesex* has a history of duplication and divergence among Paraneoptera. Three *doublesex* paralogs in *O. fasciatus* produce multiple transcripts with sex-specific and regional expression. *intersex* and *fruitless* are expressed across the body, in females and males. RNA interference reveals only one *doublesex* paralog functions in somatic sex determination. Knockdown of *doublesex* inhibits adult development of the genitalia and produces intersex phenotypes in two other sexually dimorphic structures: curvature of the fourth abdominal sternite and abdominal pigmentation. RNAi targeting *fruitless* and *intersex* also affect the genitalia of both sexes, but have affects limited to different sexually dimorphic structures in different sexes. These results reveal sex determination roles for *intersex* and *fruitless* distinct from their orthologs in other insects, and illuminate a novel form of developmental diversity in insect sex determination.

# Introduction

Sexual dimorphisms are wide-spread among animals, but their development has been studied in only a small number of species. These genetic model organisms have revealed a surprising degree of diversity in sex determination mechansisms (Schütt and Nöthiger, 2000; Kopp 2012; Herpin and Schartl, 2015), despite the deep evolutionary conservation of sex itself. However, sexual dimorphisms across the body are typically assumed to share similar regulation. Even in insects, where somatic sex determination is cell autonomous, similar mechanisms have traditionally been thought to control sex-specific differentiation in multiple tissues and organs (Arbeitman et al. 2004; Rideout et al. 2010; Robinett et al. 2010; Tanaka et al. 2011).

Somatic sex determination requires an initial genetic signal, which varies greatly from species to species. Proteins downstream of this signal then regulate transcription sex-specifically. The best-studied model of insect sex determination is *Drosophila melanogaster*, where a system of female and male chromosomal determinants reside on the X chromosome and autosomes, respectively (Baker and Ridge 1980). Thus, the proportion of X chromosomes to autosomes indirectly determines sex. Sex-specific expression and splicing of downstream genes control female and male sexual differentiation, dosage compensation, and courtship behaviors (Burtis and Baker 1989; McKeown 1992; Kelley et al. 1995; Demir and Dickson 2005; Butler et al. 2018).

Developmental regulatory genes tend to have a high degree of epistasis and pleiotropy, which limit their evolutionary divergence over time due to stabilizing selection (Stern and Orgogozo, 2009). Sex determination pathways provide an intriguing exception to this pattern, with substantial variation, even among Holometabola (Schütt and Nöthiger, 2000; Salz et al. 2011; Herpin and Schartl, 2015). *doublesex* (*dsx*) acts relatively downstream of a gene network, including *Sex-lethal* and *transformer* in *D. melanogaster* sex determination, where alternative splicing produces sex-specific transcription factor isoforms resulting indirectly from X chromosome dosage (Erickson and Quintero 2007). Dsx is notable for being conserved in its structure and function in other insects (Schütt and Nöthiger, 2000; Shukla and Nagaraju 2010; Geuverink & Beukeboom 2014; Herpin and Schartl, 2015). Alternative splicing of *dsx* is a consistent mechanism, which produces protein isoforms that orchestrate a cascade of sex-specific gene expression (Burtis and Baker 1989; Kopp 2012). The Dsx-ortholog encoded by *Dmrt1* is one of the few genes identified from insects that also has a conserved funcation in mammalian sex determination. In mice *Dmrt1* is required for testes development and male fertility (Raymond et al. 2000; Matson et al. 2011).

Here, we report the study of somatic sex determination in the milkweed bug *Oncopeltus fasciatus* (Heteroptera: Lygaeidae), focusing on *doublesex* paralogs and two sex determination

genes with divergent functions: *intersex* (*ix*) and *fruitless* (*fru*). The true bugs are a diverse and species-rich hemimetabolous order that diverged from holometabolous insects more than 370 million years ago (Misof et al. 2014). We find that *doublesex* paralogs diversified at the base of Paraneoptera, but three paralogs are maintained in Heteroptera, with only one required for somatic sexual dimorphisms in *O. fasciatus.* Milkweed bug females and males differ in the structure of the genitalia, in the curvature of the fourth abdominal sternite, and in the distribution of abdominal melanization (Fig 1). Previous research has shown that while *ix* is only required for somatic sexual dimorphism in female *D. melanogaster* (Garrett-engele et al., 2002), it is required during genitalia development in females and males of *O. fasciatus* (Aspiras et al. 2011). Surprisingly, we also find a major role for *fru* in development of both female and male sexually dimorphic structures. While there is a common requirement for *dsx* activity in all sexually dimorphic structures in *O. fasciatus*, different dimorphic traits require distinct combinations of these genes. These findings indicate that the sex determination pathway of milkweed bugs has diverged significantly from that of other insects.

# Results

## ***doublesex* paralogs in Paraneoptera**

To examine the determination of somatic sexual dimorphisms in *O. fasciatus*, we cloned several candidate genes based on genetic models from *D. melanogaster* (Arbeitman et al. 2004), including *dsx*, *ix* and *fru*. *dsx* is a key regulator of sex determination in many holometabolous insects (Garrett-engele et al., 2002; Herpin and Schartl, 2015; Schütt and Nöthiger, 2000; Geuverink and Beukeboom 2014). *ix* is required for genitalia development in both sexes in *O. fasciatus* (Aspiras et al. 2011) but only in females of *D. melanogaster* (Garrett-engele et al., 2002). In *D. melanogaster,* the transcription factor encoded by *fruitless* (*fru*) is required for sexually dimorphic brain development, necessary for male courtship behavior (Hall 1978; Demir and Dickson 2005; Ryner et al., 1996). Single copies of *ix* and *fru* were isolated from *O. fasciatus* (Fig 2A). Transcriptome and genome sequences also supported single instances of these genes. However, three genomic loci have sequence similarity to *D. melanogaster dsx* (Fig 2A). We used phylogenetic inference to verify orthology and to explore the relationships of these genes (Fig S1-S3). We found single orthologs of *ix* and *fru* in most available insect genomes, and phylogenies based on their aligned amino acid sequences mostly reflect relationships among high level insect taxa (Fig S1-S2).

In contrast, the Dsx phylogeny does not recapitulate most taxonomic relationships. Single *dsx* orthologs were recovered from holometabolous insect genomes, but multiple sequences with similarity to *D. melanogaster dsx* were found in the genomes or transcriptomes of most Paraneoptera. These sequences clustered by paralog-group, and topologies within groups

reproduced some high level taxonomic relationships (Fig S3). We refer to the clade containing holometabolous *doublesex* sequences as the *dsx* clade, and the *O. fasciatus* sequence it contains as *dsx*. We dub the sibling clades *doublesex-like-a* (*dxxa*) and *doublesex-like-b* (*dxxb*). The *dsx* and *dxxb* clades are supported in more than 80% of bootstrap replicates. Throughout this report, we will use "*doublesex*" to refer to the broader group of genes with homology to *D. melanogaster doublesex*, reserving "*dsx*" to refer to genes in the clade that excludes the *dsx*-like paralogs of Paraneoptera.

## Structure- and sex-specific transcript expression

To effect sexually dimorphic development, genes are often alternatively spliced. Using rapid amplification of cDNA ends (RACE) we isolated transcripts for all candidate genes (Fig 2B). We supplemented this survey by searching available transcriptome data, but this approach did not identify any additional transcripts. Five alternative transcripts were found for *O. fasciatus dsx*, and three each for *dxxa* and *dxxb*. All transcript isoforms from each *doublesex* paralog included a DNA-binding domain in the 5' exon. A DMRTA domain was present in the downstream exons of some transcript isoforms from each paralog.

We designed exon-specific primers to examine the expression of these transcripts using qRT-PCR (Table S1). Expression was measured in tissues isolated from teneral adults. Expression of the three *doublesex* paralogs, measured from exons containing the DNA-binding domain, showed significant correlations with one another (Spearman's rank correlation, $rho > 0.6$, $p < 10^{-5}$). Expression of *doublesex* paralog transcripts was generally low compared to other genes, and showed considerable variation by sex, tissue and exon (Fig 2C). While our primer sets do not allow unambiguous identification of transcripts in all instances, some determinations about transcript-specific expression can be made from these data.

Expression of *dsx* was generally higher in females (Fig 2C). Transcript isoform D, which contains exon 6, was the most abundant isoform, with particularly strong expression in the ovaries and ovipositor. We also detected this transcript in the male genital capsule, albeit at lower levels. Isoforms of *dsx* containing the conserved DMRTA domain were not detected in testes, but were expressed at low levels in the ovaries. *dxxa* was not detected in any male tissues, but showed relatively consistent, low expression in female tissues, excluding the ovipositor. We failed to detect *dxxa* exon 2, suggesting that all detectable expression in the sampled tissues reflects expression of transcript isoform B. Expression of *dxxb* was high in the gonads of both sexes, but low or undetectable in other tissues. This expression was greater in testes than in ovaries. We did not detect any expression of *dxxb* exon 4a in females, suggesting male specificity in transcript isoform B.

We also isolated transcripts from *ix* and *fru* using RACE. In contrast to *O. fasciatus doublesex* paralogs, *ix* and *fru* appeared to be expressed strongly and more uniformly across most of the

sampled tissues. In *D. melanogaster ix* is required for female somatic development and for sex-specific behavior in females and males (Nagoshi et al. 1988). The gene is transcribed in most tissues of both females and males from prepupal to adult stages (Gelbart and Emmert 2013). High levels of *ix* transcripts were detected in all sampled tissues in both sexes of *O. fasciatus* (Fig 2C). Expression was highest in the female ovipositor.

*fruitless* is expressed much more strongly in male than in female *D. melanogaster*, particularly in older males (Gelbart and Emmert 2013) where it is required for courtship behavior, fertility, and minor anatomical features specific to males (Hall 1978; Hall 1994; Usui-Aoki et al. 2000). Expression of *fru* in *O. fasciatus* was detected in all sampled tissues, except for the female ovipositor. Expression was strongest in the testes. Interestingly, *fru* expression was comparable and moderate in the heads of females and males (Fig 2C).

These patterns of expression for *ix* and *fru* in the milkweed bug are notably less sexually dimorphic than their orthologs in the fruit fly. Excluding the ovipositor, *fru* and *ix* show a strong correlation in expression (Spearman's rank correlation *rho* = 0.39, $p = 0.00819$). We tested for gene interactions by measuring gene expression in an RNA interference (RNAi) background. Expression of *fru* was significantly reduced in the bodies of *ix* RNAi males, compared to control males (Fig S5; Wilcoxon rank sum test, $p = 0.019$). This implies that *ix* promotes *fru* expression, although this effect may be indirect. The absence of *fru* expression in the ovipositor (Fig 2C), where *ix* is highly expressed, suggests the action of an unidentified suppressor in that context.

## Development of female and male genitalia requires *ix*, *fru* and *dsx*

To investigate the developmental functions of *ix*, *fru*, and the *doublesex* paralogs in *O. fasciatus*, we performed juvenile-stage RNAi targeting each gene, as well as a simultaneous knockdown of all *doublesex* paralogs (Tables S2, S3). We then examined sexually dimorphic traits in the resulting adults to evaluate loss-of-function phenotypes (Fig 3-4).

Among *doublesex* paralogs, knockdown of *dxxa* and *dxxb* failed to produce any discernible phenotype. There was no significant difference in genitalia length, in curvature of the A4 sternite, or in the distribution of abdominal melanism among putative females and males in RNAi treatments targeting these genes (Fig 4). However, *dsx* knockdown significantly affected development of all sexually dimorphic structures in presumptive females and males. Only dsRNAs targeting the exon containing the DNA-binding domain resulted in phenotypic changes (Table S3). This exon is present in all transcript isoforms produced from the *dsx* locus (Fig 2B). Presumptive female *dsx* RNAi specimens developed ovipositors that were significantly shorter than unmanipulated specimens (Fig 4A) and appearing reduced overall, but particularly in the distal valvulae (Fig 3R-S). The claspers of presumptive males were also dramatically shorter or

absent entirely in some specimens (Fig 3T; 4B). Male *dsx* RNAi individuals often died while molting to adulthood, when the genital capsule did not complete molting.

We also tested combined knockdown of all *doublesex* paralogs, by co-injection of three dsRNAs and by injection of a single dsRNA containing tandem sequences from the DNA-binding domain of each gene. The phenotypes of these treatments were similar to that of *dsx* RNAi alone (Fig 4). Lengths of ovipositors and claspers were significantly reduced in simultaneous knockdown of *dsx*, *dxxa* and *dxxb*, compared to controls. The magnitude of this effect was comparable to the *dsx* RNAi treatment (Fig 4).

In *D. melanogaster* the female isoform of Dsx interacts with the protein encoded by *ix* to activate female-specific target gene expression (Garrett-Engele et al. 2002). Therefore, we tested *ix* function during *O. fasciatus* development. Knockdown of *ix* by RNAi produced intersex phenotypes (Fig 3F-J; 4A-B,H), although it was still possible to identify bugs unambiguously as female and male based on the number of terminal appendages and the presence of a genital capsule in presumptive males. Length was significantly reduced in ovipositors and claspers of *ix* RNAi specimens (Fig 4A-B). Distally the ovipositor developed with heavy sclerotization, suggesting partial transformation toward a clasper-like identity (Fig 3H-I). In presumptive males, the genital capsule and claspers were significantly reduced in size (Fig 3J; 4B).

The transcription factor encoded by *fru* is conserved among insects (Fig S2). In *D. melanogaster* *fru* is required for male-specific behaviors, but plays a relatively minor role in anatomical development (Ryner et al. 1996). Surprisingly, knockdown of *fru* in *O. fasciatus* caused dramatic defects in sexually dimorphic adult structures (Fig 3K-O), similar in many ways to the effects of *dsx* and *ix* knockdowns. *fru* RNAi significantly reduced the length of the ovipositor and claspers (Fig 4A-B). While the ovipositors of *ix* RNAi specimens decreased in length, they also increased in thickness and pigmentation, suggestive of partial transformation to clasper identity. In contrast, the ovipositors of *fru* RNAi specimens did not appear transformed, and retained a membranous structure (compare Fig 3H-I to Fig 3M-N). Some presumptive female *fru* RNAi specimens also showed necrosis of the distal valvulae (Fig 3N). In *fru* RNAi males, claspers were reduced in size (Fig 4B) and often misshapen, lacking their characteristic arch (Fig 3O).

## *dsx* inhibits intersex sternite shapes in females and in males

One of the most obvious sexual dimorphisms in milkweed bugs is the posterior projection of the fourth abdominal sternite (Fig 1A). We examined the effects of RNAi gene knockdown on sternite curvature, quantified using nine landmarks placed on the sternite's posterior edge (Fig 1A-B). After Procrustes alignment of the coordinate positions, these landmarks were regressed to a line. The square-root of the mean of squared residuals (residual mean standard deviation) was used as a metric of curvature. (See Materials and Methods for more details.) Sternite curvature is not a binary trait in milkweed bugs. Females and males display a continuous range of curvature

228 (Fig 4D-F). Nevertheless, among dsRNA control specimens, the sternites of females and males
229 showed significantly different median curvatures (Wilcoxon rank sum test, $p < 2.2\times10^{-16}$).

230 Male milkweed bugs retain a juvenile sternite shape, while the female sternite projection arises
231 during the last two molts before adulthood. Therefore, we predicted that inhibiting genes
232 required for the development of sexual dimorphism might cause presumptive females to also
233 retain the juvenile sternite shape. Surprisingly, *dsx* RNAi produced sternite shape changes in
234 female and in male bugs. As expected for females, sternite curvature in *dsx* RNAi presumptive
235 females was significantly reduced compared to that of dsRNA control females (Fig 4D;
236 Wilcoxon rank sum test, $p = 4.73\times10^{-3}$). However, among presumptive male *dsx* RNAi
237 specimens, sternite curvature increased ($p = 1.12\times10^{-7}$), adopting a more typically female
238 phenotype. A similar effect of less magnitude was also produced by the simultaneous
239 knockdown of all three *doublesex* paralogs (females: $p = 0.0458$; males: $p = 4.15\times10^{-3}$). Thus, for
240 both sexes, *dsx* RNAi caused sternite shapes to become more intermediate.

## 241 Development of female sternite shape requires *fru*

242 Since knock-down of *ix* and *fru* produced dramatic phenotypes in the genitalia of female and
243 male milkweed bugs, we also examined other sexually dimorphic traits in these specimens.
244 RNAi targeting *ix* did not significantly affect the sternite curvature (Fig 4D-E). Even specimens
245 with dramatic intersex genitalia still displayed sternite curvatures typical of their presumptive sex
246 (Fig S6). In contrast, knockdown of *fru* reduced the curvature of sternites in females ($p =$
247 $0.0107$). While some presumptive female *fru* RNAi specimens had sternites with a typically male
248 shape, most developed with an intermediate curvature (Fig 4D). However, presumptive male *fru*
249 RNAi specimens were not different from dsRNA control specimens (Fig 4E; $p = 0.831$). This
250 suggests that *fru* activity is required for the increased curvature of the A4 sternite in females, but
251 not in males, which retain a more juvenile sternite shape.

## 252 Sex-specific distribution of abdominal melanism requires *dsx*

253 The ventral abdomen of *O. fasciatus* typically has several areas of melanic pigmentation. While
254 considerable individual variation exists, females and males have distinct (non-overlapping) ratios
255 of melanism on the fifth and fourth abdominal segments (Fig 4G-I). Females have less melanism
256 on A5, compared to males where melanic pigmentation is more similar on A4 and A5. Within
257 each sex, this trait is independent of the curvature of the A4 sternite (Fig S7; Spearman's rank
258 correlation for females *rho* = -0.079, $p = 0.72$; for males *rho* = -0.279, $p = 0.220$).

259 RNA interference targeting *dsx* affected the distribution of abdominal melanism in both sexes
260 (Fig 3P-Q, 4G-I). Females normally have much less melanic pigmentation on the fifth abdominal
261 sternite, compared to the fourth. However, presumptive female *dsx* RNAi specimens had
262 significantly more even distribution of melanism than control females (Wilcoxon rank sum test,

$p = 2.19\times10^{-4}$). Conversely, presumptive male *dsx* RNAi specimens had a reduction in the ratio of A5 to A4 melanic area, compared to male *AmpR* RNAi specimens ($p = 7.62\times10^{-7}$). In contrast to control specimens, where the ratio of abdominal pigmentation is completely non-overlapping, there is no longer any sexual dimorphism in this trait among *dsx* specimens ($p = 0.25$). Similar intersex phenotypes are produced by RNAi targeting all three *doublesex* paralogs (for presumptive females $p = 7.83\times10^{-5}$; for males $p = 9.47\times10^{-4}$).

### *ix* is required in males for sex-specific abdominal melanism

As with sternite shape, we also examined abdominal pigmentation following RNAi targeting *ix* and *fru*. While *fru* RNAi produced significant changes in the sternite shapes of presumptive females (Fig 4D), these specimens did not differ significantly from controls in their distribution of abdominal melanism (Fig 4G; $p = 0.41$). RNAi targeting *ix* did affect abdominal pigmentation, but only in presumptive males. Often presumptive male *ix* RNAi specimens had reduced pigmentation on the fifth abdominal segment, leading to a more typically female pigmentation pattern (Fig 4H) that was significantly less evenly distributed than in control male bugs ($p = 0.0173$).

## Discussion

### Sexual dimorphism requires *dsx*

Our results suggest a general role for *dsx* in the development of adult sexual dimorphisms in *O. fasciatus*. All three of the sexually dimorphic traits examined in this study require *dsx* function. The activity of the paralogs, *dxxa* and *dxxb*, seems to be dispensable, at least for these traits, as RNAi targeting *dxxa* and *dxxb* individually failed to produce significant deviations from the phenotypes of control specimens.

Interestingly, the function of *dsx* was not simply to promote the development of sexually dimorphic traits. Genitalia are the most obviously dimorphic structures differing in females and males, and in these appendages *dsx* RNAi reduced their length in all individuals (Fig 4A-B). However, RNAi knockdown of *dsx* produced more female-like sternite curvature in males and more male-like curvature in females, suggesting that *dsx* acts in each sex to inhibit intersex phenotypes. In effect, *dsx* makes the distribution of sternite curvature more bimodal. Each of these traits develops from a null state in juveniles. Males retain the relatively uncurved juvenile sternite shape, while neither sex has abdominal melanism as a juvenile. If the role of *dsx* was to promote sternite curvature, then we would expect male *dsx* RNAi specimens to be comparable to control males. Similarly, if *dsx* promoted abdominal pigmentation, we might expect reduced pigmentation overall with no significant effect on its distribution. However, both these traits are

more intersex in their value following *dsx* RNAi. It is likely that distinct isoforms of Dsx act on distrinct target genes to produce different effects in each sex, and that these intersex phenotypes arise from the absence of this regulation.

## Sexual dimorphisms develop by distinct mechanisms in milkweed bugs

Both female and male *O. fasciatus* require *ix* and *fru* for proper development, but in different traits (Fig 4C,F,I). Orthologs of these genes in *D. melanogaster* have much more limited roles, affecting only one sex or the other. Interestingly, while *ix* and *fru* affect genitalia development in both sexes of *O. fasciatus*, these genes affect different sexually dimorphic traits, in different sexes.

*fru* RNAi only affected the development of female, but not male, sternite curvature (Fig 4D-F). Because male sternite curvature closely resembles the phenotype of juveniles, it is possible that *fru* is involved in regulating growth and proliferation of these cells, rather than in directly determining sexually dimorphic identity. Knockdown of *ix* did not significantly change sternite curvature, but affected the distribution of abdominal pigmentation only in male milkweed bugs (Fig 4G-I). It is possible that only some Dsx isoforms in *O. fasciatus* interact with Ix, in a structure-specific context, rather than in a sex-specific context. Isoform D of *O. fasciatus dsx* is a strong candidate for this interaction, because of its strong expression in both female and male genitalia, but lower expression in other somatic body regions (Fig 2). Confirmation of this hypothesis must await the development of isoform-specific antibodies from milkweed bug Dsx. Additionally, it is possible that the expression of distinct *dsx* isoforms is regulated by tissue-specific enhancers. A recent study of regulatory sequences in *D. melanogaster* found that expression of *dsx* in distinct sexually dimorphic structures is controlled by separate enhancers (Rice et al. 2019). Similarly, analysis of gene expression in different larval and pupal tissues of the butterfly *Papilio polytes* has suggested distinct tissue-specific targets of *dsx* activity (Deshmukh et al. 2020).

These findings support the concept that some aspects of sex determination in insects may be structure-specific. In fact, it is possible that this form of regulation may be an evolutionary intermediate. If a gene has multiple enhancers for expression in different areas, as exemplified by *D. melanogaster dsx*, then a mutation eliminating one enhancer would produce the kind of mosaic genetic requirement seen for *O. fasciatus ix* and *fru.*

## Evolution of *doublesex* in Paraneoptera

The presence of multiple *doublesex* paralogs suggests an ancient gene radiation early in the diversification of Paraneoptera. The genomes of early-branching insect lineages appear to contain only one *doublesex* gene, which all clustered with the clade that includes *D. melanogaster dsx* (Fig S3). This result is consistent with two duplication events in the lineage

leading to Heteroptera. Paraneopteran *dsx* sequences had relatively long branches, suggesting that they underwent greater diversification after the duplications that produced the *dxxa* and *dxxb* paralog groups. The absence of obvious external phenotypes for *dxxa* or *dxxb* RNAi suggests that these genes have diverged from *dsx* in their function. Four *doublesex* paralogs have been identified in the brown planthopper *Nilaparvata lugens* (Hemiptera: Delphacidae). However, like *O. fasciatus*, only one *N. lugens* paralog, nested in the *doublesex* paralog group (Fig S3), has a functional requirement during somatic sex determination (Zhuo et al. 2018). Nevertheless, the persistence of the *doublesex*-like paralogs over more than 290 million years (Misof et al. 2014) suggests a critical function. We found *dxxa* expression exclusively in female *O. fasciatus*, while *dxxb* was highly expressed in testes (Fig 2C). These patterns may suggest sex-specific roles for these genes in development of the gonads, in the germline, or in other traits not examined by this study. We examined the gonads of RNAi specimens but found no obvious phenotypic differences at the anatomical level (Fig S8). Future studies will be necessary to test whether *dxxa* or *dxxb* have roles in other traits.

## Evolution of sex determination mechanisms in insects

Sex determination pathways evolve rapidly and differ substantially among animals (Herpin and Schartl, 2015; Kopp, 2012; Schütt and Nöthiger, 2000). Additionally, changes in alternative splicing and the interactions of genes, as well as their expression patterns, are mechanisms by which these pathways evolve (Baker, 1998; Salz, 2011; Shukla and Nagaraju 2010). The results we present here further illuminate the rapid evolution of sex determination genes and offer insight into the sex determination mechanisms of hemimetabolous insects.

Compared to other genes in insects involved in sexually dimorphic development, such as *ix* and *fru, doublesex* orthologs evolve rapidly in their protein sequence and have undergone multiple duplications in different lineages (Fig S3). This could suggest that *dsx* occupies a space in the developmental network where mutations are more readily tolerated. Other genes, including *ix* and *fru,* may be more limited in the evolution of their protein sequences by stabilizing selection, perhaps due to greater pleiotropy. However, differences in the functions of these genes among insect species suggest that regulatory changes still occur without comparable constraints.

The functions of *ix* and *fru* in *O. fasciatus* are different from those reported in other insects. In *D. melanogaster, ix* is only required in females for genitalia development while both female and male milkweed bugs require *ix* for genitalia development (Aspiras et al, 2011; Fig 3-4). *ix* RNAi knockdown in *N. lugens* produced genitalia defects in females, but not in males (Zhang et al. 2021). *fru* is a transcription factor required for development of male-specific neurons in *D. melanogaster* (Hall 1994; Ryner et al. 1996; Demir and Dickson 2005). In *O. fasciatus*, we find a more expansive requirement for *fru* in female and male genitalia development (Fig 3-4) and in the development of female sternite curvature (Fig 5). To the best of our knowledge, such a

prominent function for *fru* outside the nervous system has not been previously reported. Further studies of *fru* outside drosophilids are needed to better understand its functional diversity across the insects and to determine when during drosophilid evolution it became restricted to the nervous system. Overall, these differences in the functions of *ix* and *fru* suggest that somatic sex determination may have a much greater diversity of mechanisms among insects than is currently understood.

## Conclusions

In insects such as the fruit fly, *dsx* functions as a critical downstream regulator of somatic sex determination (Arbeitman et al. 2004; Kopp 2012). Our results are not consistent with this role for *dsx* in *O. fasciatus*. We did not detect sex-specific transcript isoforms of *dsx*, although expression was female-biased. Similarly, in the sweet potato whitefly, *Bemisia tabaci*, a single *dsx* ortholog also has sex-biased expression (Guo et al. 2018). Although in that member of the Sternorrhyncha, *dsx* is more strongly expressed in males and RNAi knockdown revealed a requirement in male genitalia development, and merely a role in vitellogenin regulation in females. The expression of *dxxa* in *O. fasciatus* was limited to females and high in ovaries, while expression of *dxxb* was high in testes. Similarly, *dsx* isoforms containing the DMRTA domain were only detected in ovaries, not testes. While gonads of RNAi specimens did not display anatomical defects (Fig S8), these expression patterns suggest that duplication and sex-specific divergence of these genes and transcripts may play a role in sex-specific development of the germline in *O. fasciatus*. Knockdowns of *dsx* or all three *doublesex* paralogs during juvenile development do not completely eliminate adult sexual dimorphism. Rather, *dsx*, together with *ix* and *fru*, appears to help facilitate trait-specific development of sexual dimorphisms, including the development of female and male genitalia and the inhibition of intersex values for sternite curvature and abdominal pigmentation of both sexes. Nevertheless, it is likely that unidentified genes play a more proximate role in milkweed bug sex determination.

More generally, these results show that genes may act to control the development of somatic sexual dimorphisms by acting in tissue-specific as well as sex-specific contexts. The sex determination cascades of other insects should be investigated in more detail to expand our understanding of the evolution and diversity of sex determination mechanisms. Such studies will broaden our perspective on developmental pathway evolution and help us better understand how genetic networks bias evolutionary outcomes.

# Materials and Methods

## Insect culture

*Oncopeltus fasciatus* were obtained from Carolina Biological Supply Company and maintained as described by Liu and Kaufman (2009). Milkweed bug cultures were kept in terraria at room temperature (21-23˚C) and fed on sunflower seeds. Loose cotton balls provided an egg-laying substrate. Water was provided in flasks with paper towel wicks.

## Sequence orthology

An ortholog of *ix* from *O. fasciatus*, GenBank accession AEM16993, was identified as part of a previous study (Aspiras et al. 2011). Sequences with similarity to *fru* and *dsx* were obtained from *O. fasciatus* using degenerate PCR and RACE and by PCR with exact primers based on the available genome and gene set annotation (Ewen-Campen et al. 2011; Panfilio et al. 2019). Initial identification was based on tBLASTn search using sequences from *D. melanogaster*. One genomic locus had high similarity to *fru*, while three genomic loci closely resembled *dsx*.

Orthology was confirmed using phylogenetic inference. Additional orthologs from insects were obtained from GenBank using BLAST. Alignments of amino acid sequences were performed by ClustalW in Geneious Prime (version 2019.2.3) using a gap cost of 5 and an extension cost of 0.05 with free end gaps. Alignment of Ix and Fru included all amino acids. Alignment of Doublesex orthologs was restricted to exons containing the conserved DNA-binding domain. Phylogenies were inferred using RAxML version 8.2.11 on a multiprocessor computing cluster. Mutation rates were modeled using the BLOSUM62 matrix with a gamma distribution. The program was called as "`raxml-mpi -d -f a -x 123 -p 123 -# autoMRE -m PROTCATBLOSUM62 -s X.phy`" where `X` stands in for the alignment name. Trees were rooted with sequences from other arthropod classes for Ix, collembola for Fru, and rooted at the midpoint for Doublesex. Node supports were determined by bootstrapping.

## Isolation of mRNA isoforms

Alternative splicing of mRNAs was examined using Rapid Amplification of cDNA Ends (RACE). Initial cloning of candidate genes was done via degenerate PCR with primers designed to conserved protein domains, or with exact primers designed from publicly available transcriptome data. To obtain alternative mRNA sequences, total RNA was extracted from a mix of late fifth instars and teneral adults seperated by sex, using the PureLink RNA Mini Kit (ThermoFisher). First strand cDNA synthesis was done using the GeneRacer Kit with AMV reverse transcriptase (Invitrogen). This procedure ligates a specific DNA adapter sequence to the 5' or 3' ends of cDNAs, which are then used in PCR with gene-specific and adapter-specific

431 primers. Nested PCR was used to enrich the template pool for the target sequences. From
432 multiple independent PCRs, 120 products were isolated using gel excision and cloned using the
433 Topo-TA cloning kit (Invitrogen). Sanger sequencing and alignment confirmed 51 of these
434 clones had contiguity with potential *doublesex* paralogs. These were determined to represent 3
435 genomic loci with a total of 11 splicing isoforms (Fig 2A-B). Sequences from *O. fasciatus ix*, *fru*
436 and *doublesex* transcripts were submitted to GenBank (accession numbers MZ197788 -
437 MZ197800).

438 All *doublesex* transcripts included 5' exons containing the conserved DNA-binding domain. 5'
439 RACE using gene-specific reverse primers in more downstream exons failed to isolate other
440 transcript variants. BLAST searches of available *O. fasciatus* transcriptomes (Ewen-Campen et
441 al. 2011; Panfilio et al. 2019) using downstream exons as a query also failed to identify
442 additional transcripts.

## 443 Gene expression

444 Quantitative real-time PCR (qRT-PCR) was used to measure sex- and trait-specific expression, to
445 validate RNAi knockdowns, and to investigate potential gene interactions. Specific probe and
446 primer sets were created for multiple exons in each *doublesex* paralog. Dual-labeled probes
447 (SigmaAldrich) allowed reaction multiplexing to conserve template samples. Primers and probes
448 were designed using Primer3 in Geneious Prime and are listed in Supplemental Table 1.

449 Milkweed bugs were collected without agitation and placed at -80 °C for fifteen minutes. For
450 tissue-specific assays, specimens were dissected on ice and immediately proceeded into RNA
451 isolation. RNA was extracted following the Maxwell 16 LEV Tissue RNA Kit protocol
452 (Promega). For tissue-specific assays, RNAi validation and studies of gene interactions,
453 expression was measured in templates prepared from teneral adults. Between five and seven
454 biological replicates of each sex-by-tissue combination were measured independently. RNA was
455 stored at -80 °C. First-strand cDNA was generated from 1 µg total RNA using the iScript cDNA
456 kit (BioRad) with a poly-T primer as described in the kit's instructions. qRT-PCR was carried out
457 on a CFX96 Touch qPCR System (BioRad) using iQ Supermix (BioRad). Expression was
458 calculated from the mean of technical triplicate reactions. Each plate included four DNA
459 standards diluted from known concentrations of synthesized gene fragments (IDT gBlocks) with
460 the addition of nonspecific salmon sperm DNA (ThermoFisher). All plates included control
461 reactions with water in place of the cDNA template (no-template controls) and with total RNA in
462 place of cDNA (no-RT controls). Whenever primer sets were used on multiple plates, a
463 minimum of two templates (in addition to concentration standards) were included on those plates
464 to allow inter-plate calibration. *Elongation Factor 1-α* (*EF1-α*) was used as an endogenous
465 reference gene due to the consistency of its expression throughout development (Su et al. 2011).

466 We expected that in some tissues, certain transcripts would not be expressed. Therefore, we
467 developed a method for calculating normalized gene expression that allows zero values to be
468 determined in comparison to negative controls from the same plate. Typically, normalized target
469 gene expression is determined by subtracting the mean $C_q$ for a reference gene from the mean $C_q$
470 of the gene of interest. In such cases, zero has no special meaning. Instead, we coded all
471 measurements of gene expression as zero if they were within 0.5 cycles of any template-negative
472 controls on the same plate, and maintained that value throughout analyses. Non-zero values were
473 normalized as usual to the expression of *EF1-α*. Next, expression values were scaled, so that the
474 mean of non-zero values was standardized to 1. Finally, variance was scaled to maintain the
475 relative distance from zero of the global non-zero minimum value prior to standardization.

## 476 RNA interference

477 Loss-of-function phenotypes from RNA interference (RNAi) were used to investigate gene
478 function as previously described (Aspiras et al. 2011). Knockdown was verified by qRT-PCR.
479 Double-stranded RNA (dsRNA) encoding *Ampicillin Resistance* (*AmpR*) was used as a control
480 for dsRNA toxicity and injection mortality. This sequence was chosen because it is present on
481 the pCR-Topo4 plasmid vector used in cloning of gene fragments.

482 A synthetic gene fragment (IDT gBlock) or cloned gene fragment was used to create a PCR
483 template for the synthesis of dsRNA. PCR primers were designed with an approximately 20-bp
484 exact match to the target sequence, avoiding sequences that also occur in paralogs (Table S2). A
485 5' T7 polymerase promoter sequence was added to both primers. Following PCR, dsRNA was
486 transcribed using the T7 MegaScript Transcription Kit (ThermoFisher). Template DNA was
487 removed by treatment with DNase I. Slow cooling to room temperature allowed dsRNA
488 annealing. Samples were cleaned by precipitation in cold ethanol and ammonium acetate. The
489 product was resuspended in nuclease-free water and stored at -20 °C. Double-stranded RNA
490 structure was confirmed by a coherent band on an agarose electrophoretic gel. dsRNA
491 concentrations were measured using a nanoscale spectrophotometer. dsRNA solutions were
492 diluted in saline buffer (0.01 mM $NaPO_4$, 5 mM KCl, green food coloring) and stored at -20 °C.

493 RNAi was tested at several dsRNA concentrations (Table S3). Fourth instar *O. fasciatus* are not
494 yet sexually dimorphic. (Milkweed bugs have 5 juvenile instars.) Fourth instars were
495 anesthetized using a $CO_2$ pad and injected with dsRNA solutions using a borosilicate glass
496 microcapillary, pulled on a Sutter Instruments pipette puller into an injection needle.
497 Approximately 0.5 µl of dsRNA solution was injected into the left side of the abdomen of each
498 bug.

499 The effectiveness of RNAi was validated using qRT-PCR. Gene expression was measured in
500 control (*AmpR* dsRNA) specimens and RNAi treatments targeting the genes of interest (Fig S4)
501 in adults no more than 1 day old. Primers used for validation PCRs did not overlap with the

502 dsRNA sequences. RNAi validation of *dxxa* RNAi was not possible, because expression of *dxxa*
503 could not be detected in the whole bodies of 28 *AmpR* or 16 *dxxa* RNAi specimens examined.
504 While *dxxa* expression was detected in specific body regions of unmanipulated bugs (Fig 2C),
505 the overall expression of *dxxa* appears to be very low.

## 506 Morphometry

507 We examined three somatic sexual dimorphisms, genitalia length, sternite curvature, and
508 abdominal pigmentation patterns (Fig 1). Specimens were imaged on a VWR VistaVision
509 dissecting microscope with a Moticam 5 digital camera. A ruler was included in the image for
510 scale. The ImageJ (Schneider et al. 2012) line-tool was used to measure the length of genitalia
511 and the femur, which was used to normalize for body size. In females, the absolute length of the
512 first valvulae of the ovipositor was measured from the point of emergence to the distal tip (Fig
513 1C). For males, the segmented line-tool was used to measure clasper length from the proximal
514 joint to the tip (Fig 1D). Using the multi-point tool, nine points were placed across the posterior
515 edge of the fourth abdominal sternite (Fig 1A-B). Raw pixel values were converted to metric
516 distances based on measurement of the ruler scale in each image.

517 To quantify sternite curvature, landmark coordinate positions from each specimen were marked
518 in ImageJ and stored in the TPS format (Rohlf 2015). Coordinates were then aligned using
519 generalized Procrustes alignment, as implemented in the R package geomorph (Adams et al.
520 2020). Landmarks at the left and right sides and on the anatomical midline were fixed, but others
521 were treated as semilandmarks. Curvature was defined as the residual mean standard deviation
522 (RMSD) from a linear regression of Procrustes-aligned coordinate values. Larger RMSD values
523 indicated a higher amount of curvature in the sternite, the more characteristically female
524 phenotype.

525 Ventral abdominal pigmentation of *O. fasciatus* adults varies with sex (Fig 1A-B; 4G-I). Rearing
526 temperature can also influence pigmentation (Sharma et al. 2016). Bugs in this study were kept
527 at a consistent temperature (21 - 23˚C), limiting this environmental influence. Within 1-2 hours
528 of the imaginal molt, melanic areas are visible on the ventral abdomen. These areas were
529 quantified using the freehand selection tool in ImageJ. Pixel areas were converted to metric area
530 based on measurement of a mm scale in each photograph.

## 531 Statistical analyses

532 Gene expression and phenotypes produced through RNAi are expected to produce skewed
533 disruptions. Therefore, we used nonparametric statistical methods to analyze these data. We used
534 the Kruskal-Wallis analysis of variance to detect overall effects. Post-hoc contrasts were
535 examined using Dunn's test, for multiple pairwise comparisons of gene expression (Dinno 2017),
536 or the Wilcoxon rank sum test, for two-sample comparisons of phenotypic values. We used

one-sided tests for the comparison of sex-specific phenotypes. Where appropriate, correction for multiple tests was done using the FDR method. R version 4.0.3 was used for all statistical analyses and the ggplot2 package was used for plotting data. Figures were assembled in Adobe Illustrator.

### Data availability

DNA sequences were archived in GenBank (accession numbers MZ197788 - MZ197800). All other data were archived at Dryad ( https://doi.org/10.5061/dryad.kwh70rz3q ), including amino acid sequence alignments of candidate gene orthologs and resulting Newick tree files, tables of morphological measurements and 2D landmark coordinate positions for sternite shapes, gene expression data, and the R scripts used for analysis.

# Acknowledgements

The authors wish to thank several people for their support and comments on an early draft of the manuscript: Devin M. O'Brien, Joshua L. Steele, Lyndell M. Bade, Johanna van Oers, Russell Johnson, David L. Stern, and Cassandra G. Extavour. Special thanks to Kristen Panfilio for sharing transcriptome data prior to their publication. Research reported in this publication was supported by the Colby College Division of Natural Sciences, by an Institutional Development Award (IDeA) from the National Institute of General Medical Sciences of the National Institutes of Health under grant number P20GM0103423, and by grant IOS-1350207 from the National Science Foundation to DRA.

# References


Adams, D. C., M. L. Collyer, and A. Kaliontzopoulou. 2020. Geomorph: Software for geometric morphometric analyses. R package version 3.2.1. https://cran.r-project.org/package=geomorph.

Arbeitman, M. N., Fleming, A. A., Siegal, M. L., Null, B. H. & Baker, B. S. A genomic analysis of *Drosophila* somatic sexual differentiation and its regulation. *Development* **131**, 2007–2021 (2004). doi: 10.1242/dev.01077

Aspiras, A.C., Smith, F.W., Angelini, D.R., 2011. Sex-specific gene interactions in the patterning of insect genitalia. Dev. Biol. 360, 369–380. https://doi.org/10.1016/j.ydbio.2011.09.026

Baker, B. S. & Ridge, K. A. Sex and the single cell. I. On the action of major loci affecting sex determination in *Drosophila melanogaster*. *Genetics* **94**, 383–423 (1980).

Burtis, K. C. & Baker, B. S. *Drosophila doublesex* gene controls somatic sexual differentiation by producing alternatively spliced mRNAs encoding related sex-specific polypeptides. *Cell* **56**, 997–1010 (1989).

Demir, E. & Dickson, B. J. *fruitless* splicing specifies male courtship behavior in *Drosophila*. *Cell* **121**, 785–794 (2005).

Deshmukh, R., Lakhe, D., and Kunte, K. (2020). Tissue-specific developmental regulation and isoform usage underlie the role of *doublesex* in sex differentiation and mimicry in *Papilio* swallowtails . *R. Soc. Open Sci.* 7, 200792. doi:10.1098/rsos.200792.

Erickson, J. W., and Quintero, J. J. (2007). Indirect Effects of Ploidy Suggest X Chromosome Dose, Not the X:A Ratio, Signals Sex in Drosophila. *PLOS Biol.* 5, e332. doi:10.1371/JOURNAL.PBIO.0050332.

Garrett-Engele, C.M., Siegal, M.L., Manoli, D.S., Williams, B.C., Li, H., 2002. *intersex*, a gene required for female sexual development in *Drosophila*, is expressed in both sexes and functions together with *doublesex* to regulate terminal differentiation. Development. 129, 4661–4675. https://dev.biologists.org/content/129/20/4661.article-info

Gelbart, W.M., Emmert, D.B. (2013). FlyBase High Throughput Expression Pattern Data

583 Geuverink, E. & Beukeboom, L.W., 2014. Phylogenetic distribution and evolutionary dynamics
584 of the sex determination genes *doublesex* and *transformer* in insects. *Sexual Development*,
585 8(1–3), pp.38–49. doi: 10.1159/000357056

586 Guo, L., Xie, W., Liu, Y., Yang, Z., Yang, X., Xia, J., et al. (2018). Identification and
587 characterization of *doublesex* in *Bemisia tabaci*. *Insect Mol. Biol.* 27, 620–632.
588 doi:10.1111/imb.12494.

589 Hall, J. C. Courtship among males due to a male-sterile mutation in *Drosophila melanogaster*.
590 *Behav. Genet.* **8**, 125–141 (1978). doi: 10.1007/BF01066870

591 Hall, J. C. The mating of a fly. *Science* **264**, 1702–1714 (1994). doi: 10.1126/science.8209251

592 Herpin, A. & Schartl, M. Plasticity of gene−regulatory networks controlling sex determination:
593 of masters, slaves, usual suspects, newcomers, and usurpators. *EMBO Rep.* **16**, 1260–1274
594 (2015). https://doi.org/10.15252/embr.201540667

595 Kelley, R.L., Solovyeva, I., Lyman, L.M., Richman, R., Solovyev, V., Kuroda, M.I., 1995.
596 Expression of Msl-2 causes assembly of dosage compensation regulators on the X
597 chromosomes and female lethality in *Drosophila*. Cell 81, 867-877.
598 https://doi.org/10.1016/0092-8674(95)90007-1

599 Kopp, A., 2012. *Dmrt* genes in the development and evolution of sexual dimorphism. Trends
600 Genet. 28, 175–184, https://doi.org/10.1016/j.tig.2012.02.002

601 Liu, P. & Kaufman, T. C. Morphology and Husbandry of the Large Milkweed Bug, *Oncopeltus*
602 *fasciatus*. *Cold Spring Harb. Protoc.* **2009**, pdb.emo127-- (2009). doi:10.1101/pdb.emo127

603 Matson, C. K. *et al.* DMRT1 prevents female reprogramming in the postnatal mammalian testis.
604 *Nature* **476**, 101–105 (2011). http://www.nature.com/articles/nature10239

605 McKeown, M. Sex differentiation: The role of alternative splicing. *Curr. Opin. Genet. Dev.* **2**,
606 299–303 (1992). https://linkinghub.elsevier.com/retrieve/pii/S0959437X05802886

607 Nagoshi, R.N., McKeown, M., Burti, K.C., Belote, J.M., Baker, B.S. 1988. The control of
608 alternative splicing at genes regulating sexual differentiation in *D. melanogaster*. Cell
609 53(2):229-36. doi: 10.1016/0092-8674(88)90384-4.

610 R Core Team (2019). R: A language and environment for statistical computing. R Foundation for
611 Statistical Computing, Vienna, Austria. URL https://www.R-project.org/.

612 Rice, G. R. *et al.* Modular tissue-specific regulation of doublesex underpins sexually dimorphic
613 development in drosophila. *Dev.* **146**, (2019). doi: 10.1242/dev.178285

614 Rideout, E. J., Dornan, A. J., Neville, M. C., Eadie, S. & Goodwin, S. F. Control of sexual
615 differentiation and behavior by the *doublesex* gene in *Drosophila melanogaster*. *Nat.*
616 *Neurosci.* **13**, 458–466 (2010). doi: 10.1038/nn.2515

617 Robinett, C. C., Vaughan, A. G., Knapp, J.-M. & Baker, B. S. Sex and the Single Cell. II. There
618 Is a Time and Place for Sex. *PLoS Biol.* **8**, e1000365 (2010). doi:
619 10.1371/journal.pbio.1000365

620 Rohlf, F. J., 2015. The tps series of software. Hystrix 26, 9–12,
621 https://doi.org/10.4404/hystrix-26.1-11264

622 Ryner, L.C., Goodwin, S.F., Castrillon, D.H., Anand, A., Villella, A., Baker, B.S., Hall, J.C.,
623 Taylor, B.J., Wasserman, S. 1996. Control of Male Sexual Behavior and Sexual Orientation
624 in *Drosophila* by the *fruitless* gene. Cell 87(6), 1079-1089,
625 https://doi.org/10.1016/S0092-8674(00)81802-4

626 Salz, H.K., 2011. Sex Determination in Insects: a binary decision based on Alternative Splicing.
627 Nature 21, 395–400, https://doi.org/10.1016/j.gde.2011.03.001.Sex

628 Schneider, C. A., Rasband, W. S., and Eliceiri, K. W. (2012). NIH Image to ImageJ: 25 years of
629 image analysis. *Nat. Methods 2012 97* 9, 671–675. doi:10.1038/nmeth.2089.

630 Schütt, C., Nöthiger, R., 2000. Structure, function and evolution of sex-determining systems in
631 Dipteran insects. Development 127, 667–677, https://dev.biologists.org/content/127/4/667

632 Sharma, A. I., Yanes, K. O., Jin, L., Garvey, S. L., Taha, S. M., and Suzuki, Y. (2016). The
633 phenotypic plasticity of developmental modules. *Evodevo* 7, 15.
634 doi:10.1186/s13227-016-0053-7.

635 Shukla, J.N., Nagaraju, J., 2010. *Doublesex*: a conserved downstream gene controlled by diverse
636 upstream regulators. Journal of Genetics 89, 341-356. doi: 10.1007/s12041-010-0046-6

637 Stern, D.L., Orgogozo, V., 2009. Is Genetic Evolution Predictable? Science, 323(5915), 746-751.
638 https://doi.org/10.1126/science.1158997

639 Su, J., Zhang, R., Dong, J., Yang, C., 2011. Evaluation of internal control genes for qRT-PCR
640 normalization in tissues and cell culture for antiviral studies of grass carp
641 (*Ctenopharyngodon idella*). Fish Shellfish Immunol. 30, 830–835,
642 https://doi.org/10.1016/j.fsi.2011.01.006

643 Tanaka, K., Barmina, O., Sanders, L. E., Arbeitman, M. N. & Kopp, A. Evolution of
644 Sex-Specific Traits through Changes in HOX-Dependent *doublesex* Expression. *PLoS Biol.*
645 **9**, e1001131 (2011). doi: 10.1371/journal.pbio.1001131

646 Usui-Aoki, K., Ito, H., Ui-Tei, K., Takahashi, K., Lukacsovich, T., Awano, W., et al. (2000).
647 Formation of the male-specific muscle in female *Drosophila* by ectopic *fruitless* expression.
648 *Nat. Cell Biol.* 2, 500–506. doi:10.1038/35019537.

649 Wickham, H.. ggplot2: Elegant Graphics for Data Analysis. Springer-Verlag New York, 2016.
650 https://ggplot2.tidyverse.org

651 Zhang, H.-H., Xie, Y.-C., Li, H.-J., Zhuo, J.-C., and Zhang, C.-X. (2021). Pleiotropic Roles of
652 the Orthologue of the *Drosophila melanogaster Intersex* Gene in the Brown Planthopper.
653 *Genes.* 12, 379. doi:10.3390/genes12030379.

654 Zhuo, J.C., Hu, Q.L., Zhang, H.H., Zhang, M.Q., Jo, S.B., Zhang, C.X., 2018. Identification and
655 functional analysis of the *doublesex* gene in the sexual development of a hemimetabolous
656 insect, the brown planthopper. Insect Biochem. Mol. Biol. 102, 31–42,
657 https://doi.org/10.1016/j.ibmb.2018.09.007

# 658 Figure Legends

659 **Figure 1**

660 **Milkweed bugs have several sexually dimorphic features.** (A-B) The fourth abdominal body
661 segment (A4) of females has an exaggerated extension of the sternite at the ventral midline. Nine
662 landmarks were placed along the ventral edge of the sternite to quantify curvature. (C)
663 Appendages from the terminal segments of the female abdomen form an ovipositor. Ovipositor
664 length was measured from the distal tip to the proximal joint. (D) The male abdomen ends in a
665 large genital capsule, which contains the copulatory organ. Externally a pair of small claspers,
666 visible from a posterior perspective, is used for mate guarding. Clasper length was measured
667 from the proximal joint to the tip.

668 **Figure 2**

669 **Structure and expression of candidate sex determination genes in *O. fasciatus*.** (A)
670 Orthologs of *intersex*, *fruitless*, and three *doublesex* paralogs were identified on different

genomic scaffolds in the *O. fasciatus* genome. Boxes represent exons; angled lines represent introns. Introns were very long compared to neighboring gene predictions. Flags indicate the start of transcription. (B) Transcripts from *ix*, *fru* and *doublesex* paralogs. The first exon of each transcript is aligned at the left. Omitted exons are left empty. Alternative start or stop sites for exons are indicated by lowercase letters (e.g. 2a, 2b) Lighter shading indicates UTRs. (C) A heatmap showing relative transcript abundance from five body regions in each sex. Each panel represents the mean of 5 to 7 independent measurements. Global differences in means were tested using the Kruskal-Wallis rank sum test. Where differences were significant, Dunn's test of multiple comparisons using rank sums was applied post hoc. Lowercase letters indicate significant differences after correction for multiple tests ($\alpha = 0.05$).

## Figure 3

**Effects of RNA interference on sexual dimorphism.** (**A-E**) Unmanipulated *O. fasciatus.* Ventral views of the female and male abdomen differ in the curvature of the fourth sternite, in the distribution of melanic pigment, and in the morphology of the genitalia. Abdomens are shown with anterior towards the top of the page (A,B). The ovipositor is a jointed structure formed by two nested appendages that end in membranous valvulae. Ovipositors are shown from ventral perspective, with anterior up (C), and from left lateral perspective, with dorsal up (D). The male genital capsule (E) is visible from a posterior view; dorsal is up. The posterior of the capsule ends in dorsally pointing claspers (white arrow), used by the male to hold onto females during and after mating. The abdominal panels share the same scale, while the ovipositor and clasper images share a separate scale. One millimeter scale bars are given for each group of panels. Strongly affected RNAi specimens are shown to illustrate phenotypes. (**F-J**) *ix* RNAi produces intersex phenotypes in females and males. The female ovipositor is reduced in length and heavily sclerotized, suggesting partial transformation toward a clasper-like identity. The male genital capsule and claspers (red arrow) are severely reduced. (**K-O**) *fru* RNAi also reduced the size of the ovipositor and claspers. Claspers are also misshapen (red arrow). (**P-T**) RNAi targeting *dsx* results in extreme reduction of terminal appendages in both sexes. Only a small nub of tissue represents the valvulae and claspers (red arrow) in severely affected specimens.

## Figure 4

**Quantification of RNAi effects** on genitalia length (A-B), sternite curvature (D-E) and abdominal melanism (G-H) in females (A,D,G) and males (B,E,H). Dots represent individual specimens. Gray outlines show the relative distribution of values. The mean of control (*AmpR* dsRNA) specimens is indicated by the horizontal line in each panel. Stars indicate significant

difference from control values, based on one-sided Wilcoxon rank sum tests with FDR correction. * $p < 0.05$; ** $p < 0.01$; *** $p < 0.001$, and are summarized beside a sketch of typically female and male phenotypes at the right (C,F,I).

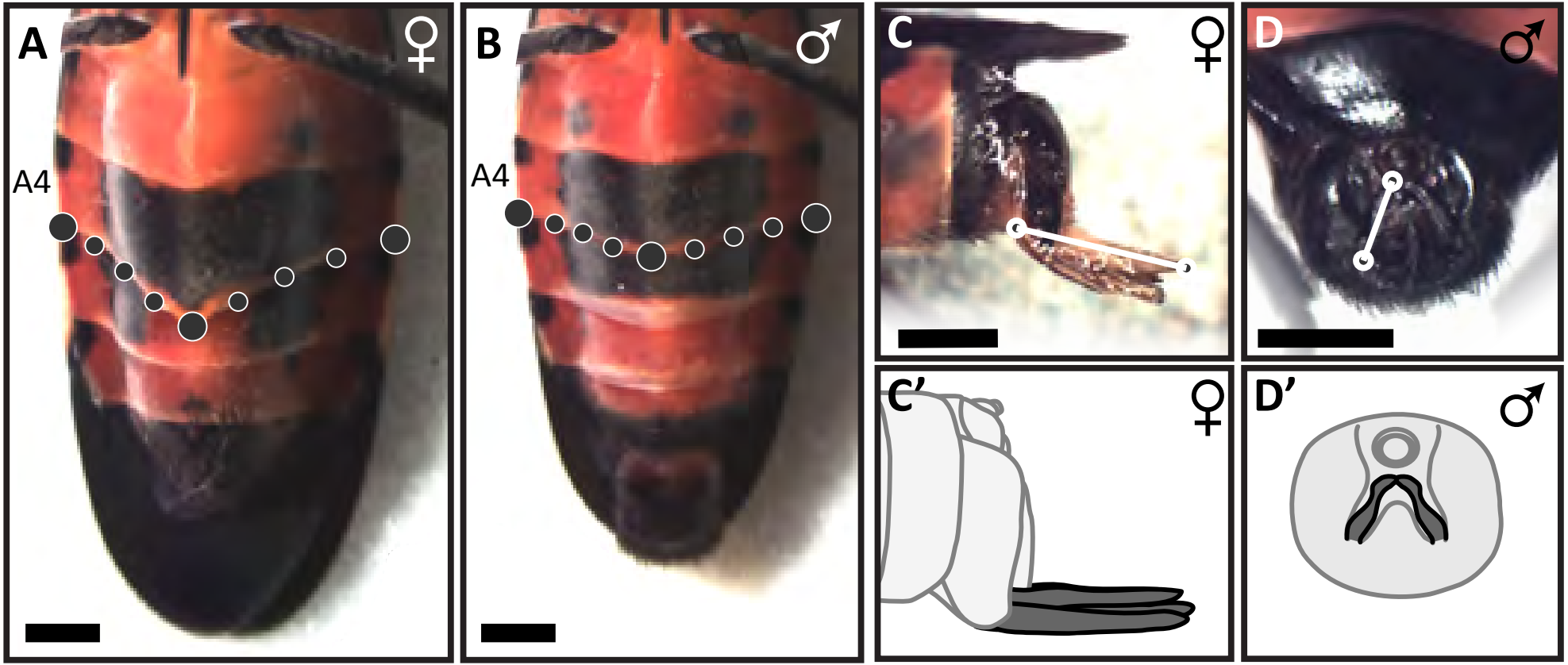
A
♀
A4
B
♂
A4
C
♀
D
♂
C'
♀
D'
♂

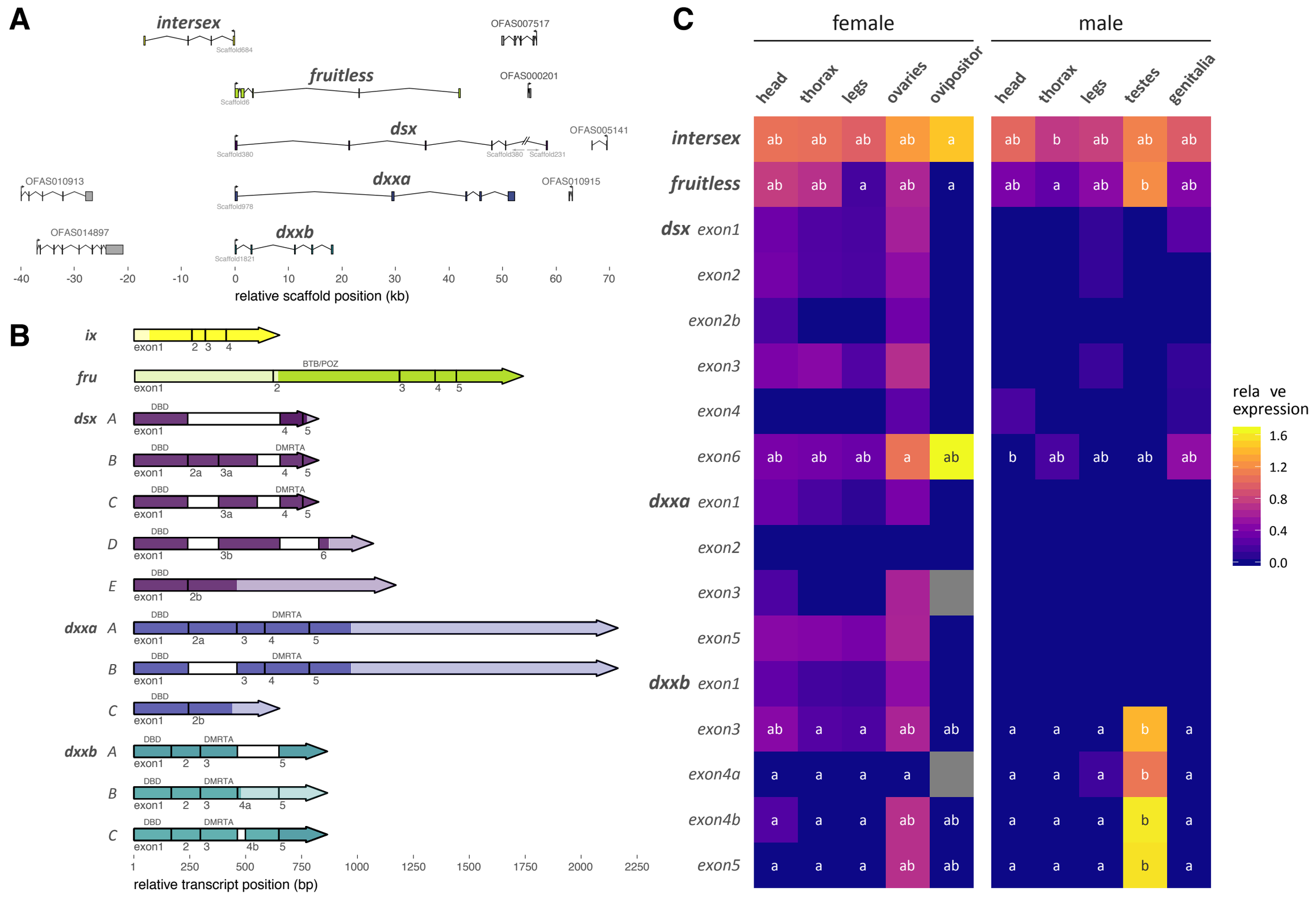
A
intersex
Scaffold684
OFAS007517
fruitless
Scaffold6
OFAS000201
dsx
Scaffold380
Scaffold380
Scaffold231
OFAS005141
OFAS010913
dxxa
Scaffold978
OFAS010915
OFAS014897
dxxb
Scaffold1821
-40 -30 -20 -10 0 10 20 30 40 50 60 70
relative scaffold position (kb)
B
ix
exon1 2 3 4
fru
BTB/POZ
exon1 2 3 4 5
dsx A
DBD
exon1 4 5
B
DBD DMRTA
exon1 2a 3a 4 5
C
DBD DMRTA
exon1 3a 4 5
D
DBD
exon1 3b 6
E
DBD
exon1 2b
dxxa A
DBD DMRTA
exon1 2a 3 4 5
B
DBD DMRTA
exon1 3 4 5
C
DBD
exon1 2b
dxxb A
DBD DMRTA
exon1 2 3 5
B
DBD DMRTA
exon1 2 3 4a 5
C
DBD DMRTA
exon1 2 3 4b 5
1 250 500 750 1000 1250 1500 1750 2000 2250
relative transcript position (bp)
C
female
male
head thorax legs ovaries ovipositor
head thorax legs testes genitalia
intersex ab ab ab ab a ab b ab ab ab
fruitless ab ab a ab a ab a ab b ab
dsx exon1
exon2
exon2b
exon3
exon4
exon6 ab ab ab a ab b ab ab ab ab
dxxa exon1
exon2
exon3
exon5
dxxb exon1
exon3 ab a a ab ab a a a b a
exon4a a a a a a a a b a
exon4b a a a ab ab a a a b a
exon5 a a a ab ab a a a b a
rela ve expression
1.6
1.2
0.8
0.4
0.0

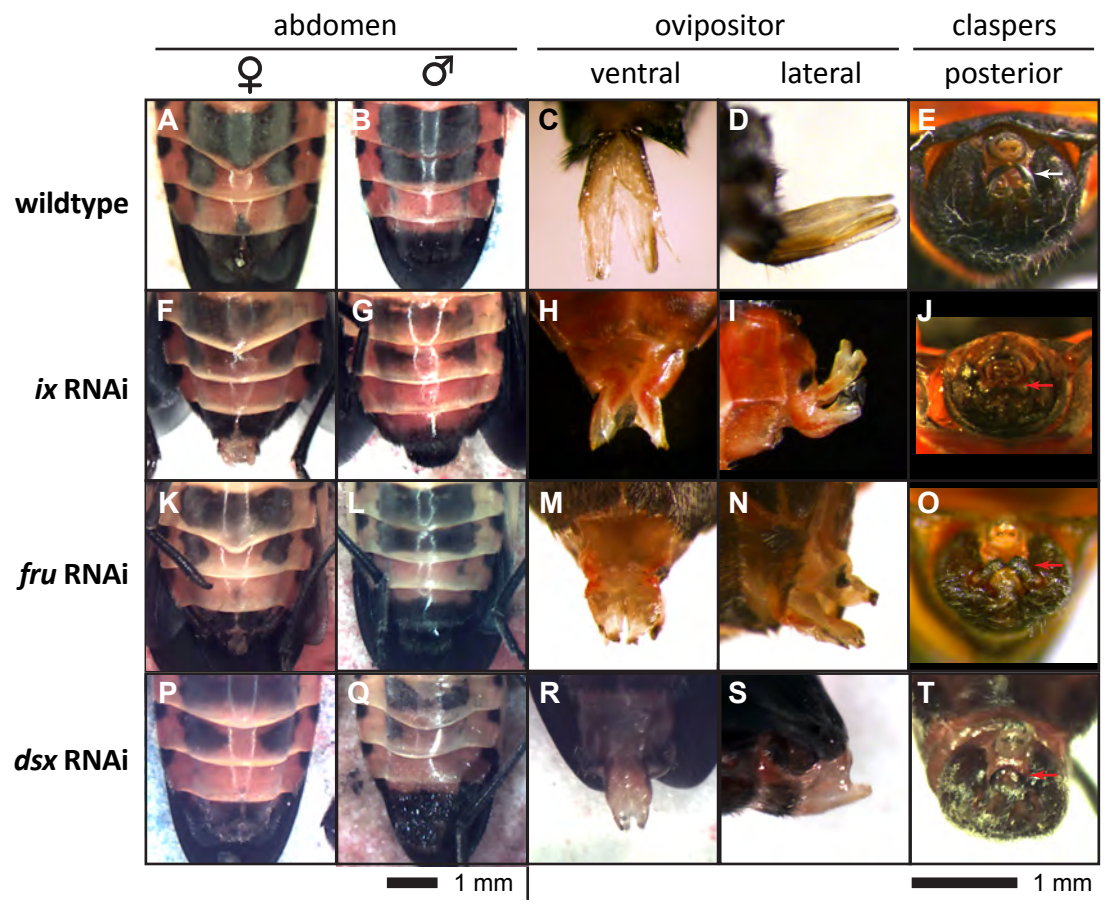
abdomen
ovipositor
claspers
♀
♂
ventral
lateral
posterior
wildtype
ix RNAi
fru RNAi
dsx RNAi
A
B
C
D
E
F
G
H
I
J
K
L
M
N
O
P
Q
R
S
T
1 mm
1 mm

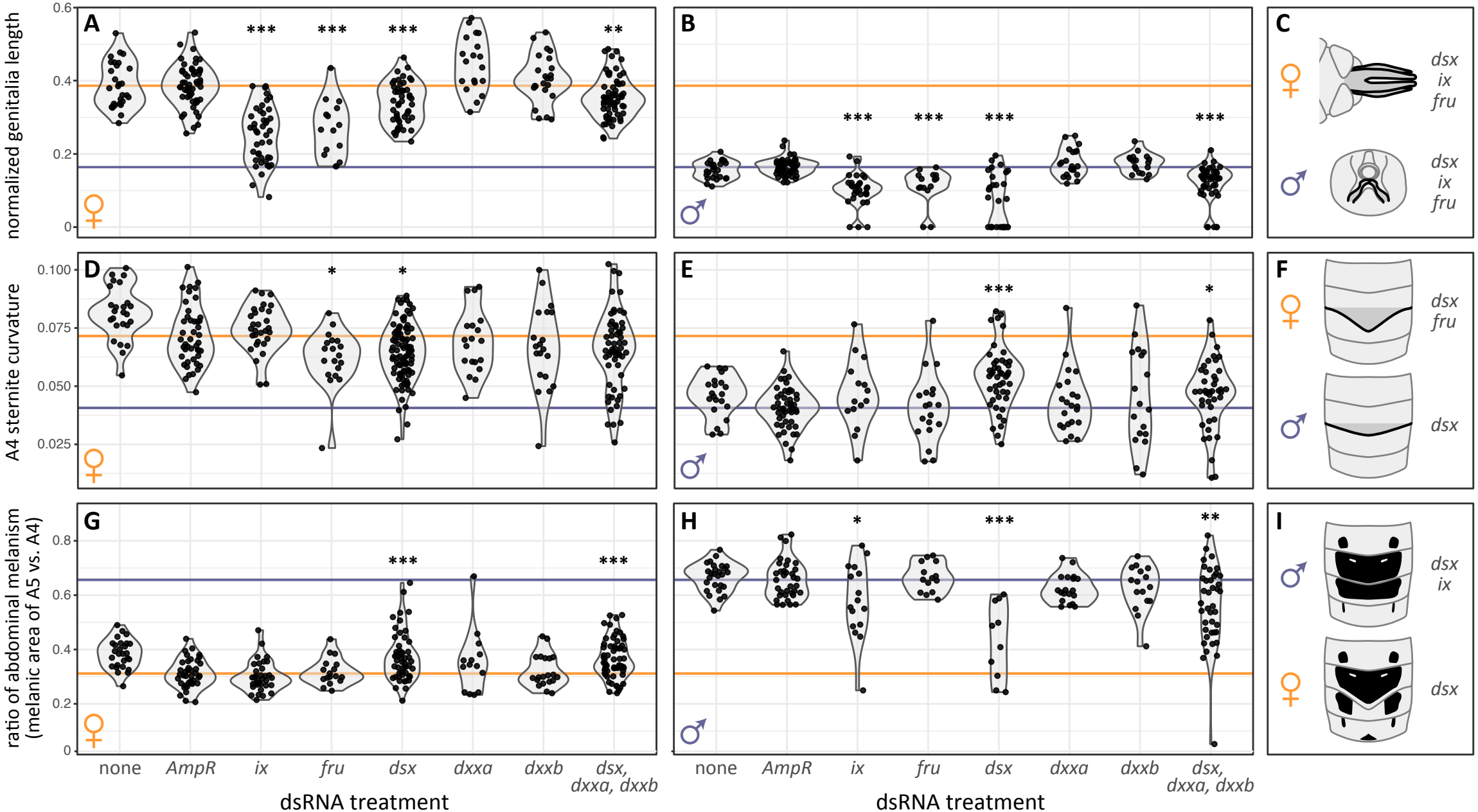
A
B
C
D
E
F
G
H
I
normalized genitalia length
A4 sternite curvature
ratio of abdominal melanism
(melanic area of A5 vs. A4)
0.6
0.4
0.2
0
0.100
0.075
0.050
0.025
0.8
***
**
*
none
AmpR
ix
fru
dsx
dxxa
dxxb
dsx,
dxxa, dxxb
dsRNA treatment
dsx
ix
fru